International Journal on Advanced Science Engineering Information Technology

Vol.11 (2021) No. 6
ISSN: 2088-5334

Effect of Thermomechanical Treatment on Mechanical Properties and Microstructure of Titanium Alloy Ti-6AL-4V ELI for Orthopedic Applications

Sir Anderson [a,b], Erit Fernando [a], Jon Affi [a], Yuli Yetri [b], Gunawarman [a,*]

[a] Department of Mechanical Engineering, Universitas Andalas, Limau Manis, Padang, 25163, Indonesia
[b] Department of Mechanical Engineering, Politeknik Negeri Padang, Padang, Indonesia
Corresponding author: [*]gunawarman@eng.unand.ac.id

Abstract— **Traffic accidents and osteoporosis significantly contribute to the incidence of fractures in Indonesia, increasing the need for orthopedic implant materials, such as titanium alloy Ti-6Al-4V ELI, which has good biocompatibility and availability in the market. However, its strength needs to be increased through thermomechanical treatment to maintain its durability. In this study, such treatment was applied with a combination of solution heat treatment at 950°C and a 1-hour holding time, followed by, subsequently, rapid cooling using water quenching, plastic deformation with deformation variations of 10%, 20%, and 30%, and aging treatment at a temperature of 550°C and holding time for 1.5 hours. The material surface microstructure was observed using an Olympus GX71 optical microscope; the chemical composition was measured using Electron dispersive X-ray, and; the hardness was measured using a Vickers microhardness tester. All data obtained were then analyzed to determine the effect of thermomechanical treatment on the increase and changes in the tested material's hardness and microstructure, respectively. The results showed that thermomechanical treatment could increase the hardness of Ti-6Al-4V ELI, as expressed by the equation HVN = 135ε + 381.5, with a correlation coefficient of 0.991. Hence, it could be concluded that thermomechanical treatment can increase the hardness of Ti-6Al-4V ELI and, finally, change its microstructure, indicating an increase in the α phase. Therefore, Ti-6Al-4V ELI treated with thermomechanical treatment can be an alternate material in orthopedic implant applications.**

Keywords—**Titanium; Ti-6Al-4V ELI; thermomechanics; solution treatment; aging treatment.**

Manuscript received 8 Apr. 2021; revised 27 Aug. 2021; accepted 28 Sep. 2021. Date of publication 31 Dec. 2021.

I. INTRODUCTION

Fracture cases in the world, including Indonesia, have continued to increase in the last few years. Most of them are caused by traffic accidents and the increasing incidence of osteoporosis in old adults. These two causes have led to an increase in the demand for orthopedic implant materials. Generally, materials used to make orthopedic implants are metals [1]. Metallic biomaterials are used as raw materials for orthopedic implants based on their characteristics, namely their good biomechanical, biochemical, and biological compatibility with the human body. Some metallic biomaterials often used as implant materials are SUS 316L stainless steel [2], Co-Cr alloys, and titanium alloys, having an elastic modulus of 200 GPa, 220-230 GPa, and 110 GPa, respectively [1], [3].

Titanium is the one that has a modulus of elasticity closer to bone (30Gpa). Ti-6Al-4V ELI is a titanium alloy widely used as an orthopedic implant material since it has a relatively low modulus of elasticity, good corrosion resistance, good biomechanical properties [4], [5], and better biocompatibility. In more detail, it has quite good mechanical properties, such as elastic modulus of 110 GPa, yield strength of 900 MPa, the maximum tensile strength of 1000 MPa, and fatigue strength of 600 MPa, thus suitable for use as an orthopedic implant material [1]. Even so, it still has challenges to its mechanical advantages since, for orthopedic implant applications, an implant must have sufficient strength to withstand the load that exists either static (in bone graft implant applications) or dynamic loads (in knee joint implant applications) [6]. Therefore, mechanical properties, such as strength, are important factors to maintain the durability of alloy materials when used as implant materials.

One way to increase the strength of the material is by giving thermomechanical treatment through a combination of heat treatment [7] and mechanical treatment that is very promising to improve the mechanical properties of titanium alloys [8]. Thermomechanical treatment is also very effective in controlling the microstructure and mechanical properties of titanium alloys. For this reason, this study applied this method to increase the strength of the titanium alloy Ti-6Al-4V ELI.

Furthermore, several studies have developed Ti-6Al-4V-based materials to be applied as orthopedic implants. Some studies analyzed the corrosion behavior of Ti-6Al-4V [9]-[53], thermomechanical processes on Al–Cu–Li alloy [54], Cu–Cr–Ag alloy [55], polycrystalline magnesium [56], and Zircaloy-4 Tubes of Mock-Up Dissolver Vessel [57], thermomechanical treatment of titanium alloy type β TNTZ by combining solution heat treatment, aging treatment, and mechanical treatment by cold rolling process [58]. Some researchers have studied a thermomechanical treatment done on titanium alloys (α+β) Ti-6Al-4V and Ti-6Al-2Mo-2Cr by combining solution heat treatment, aging treatment, and mechanical treatment with the forging process. However, they merely analyzed the effect of thermomechanical treatment on the microstructure [59]. In this research, we studied the effect of thermomechanical treatment on the mechanical properties and microstructure of titanium alloy Ti-6Al-4V ELI to obtain an implant material with optimum mechanical properties, namely good resistance when used as an alternative material for orthopedic implants. This study determined the effect of thermomechanical treatment on the mechanical properties and microstructure of titanium alloy Ti-6Al-4V ELI as an alternate material for orthopedic implants.

II. Materials And Method

A. Sample Preparation

The sample included 13 Ti-6Al-4V ELI specimens, each measuring 12 mm in diameter and 6 mm in thickness. A specimen was used for characterization test before therm[48]omechanical treatment; three were used for characterization in heat treatment without plastic deformation; while the remaining nine specimens were divided into three groups (each consisting of three) for characterization test after thermomechanical treatment with plastic deformation variations of 10%, 20%, and 30%, respectively.

The specimens were next mechanically loaded by pressing them in the axial direction at room temperature (27°C) with deformation changes of 10%, 20%, and 30% for each of the three specimens. A Takeda hydraulic press machine was used for the pressing procedure. The aging process followed, which included reheating at 550°C for 1.5 hours with also 1.5 hours holding duration. It was followed by progressive cooling at ambient temperature. Figure 1 above shows the thermomechanical process scheme.

The plastic deformation can be examined using equation (1) [60]:

$$\varepsilon = \frac{\Delta h}{ho} x\ 100\% \quad (1)$$

Δh = ho - hi

where hi is the final height (mm), ho is the initial height (mm), Δh is the change in height (mm), and ε is the plastic deformation (%). The change in height due to plastic deformation was measured using a dial indicator equipped with a magnetic stand.

B. Chemical Composition, Microstructure, and Hardness Examination

An energy-dispersive X-ray (EDX) (EMAX X-Act series) linked to a Hitachi S-3400N scanning electron microscope was used to assess chemical composition (SEM). An Olympus GX71 optical microscope was used to analyze the material's microstructure. The hardness of the material was determined using a Vicker microhardness tester (SHIMADZU HMV-1), under ASTM 384 [59]. In this test, the indenter was shaped like a four-sided pyramid at a 136° angle, a significant loading of 9.8 N, and two to fifteen seconds indentation time.

C. Thermomechanical Treatment

Solution therapy (ST), mechanical treatment, and aging treatment were used in the thermomechanical process (AT), see Figure 1. A Ney Ceramfires vacuum heating furnace was used to complete the heating procedure. Heating to 950ºC with an increased temperature at 10ºC/s and an hour holding time, followed by fast cooling using water quenching, was used to treat the solution (WQ).

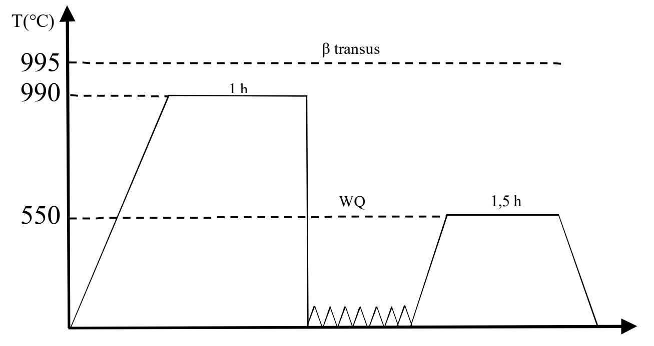

Fig. 1 Thermomechanical process scheme

D. Flowchart of Research Stages

Figure 2 shows a flow chart of this research. The implementation of this research was started by preparing Ti-6Al-4V alloy test material, which began from cutting the sample into size according to the specified dimensions. After that, microstructure examination, chemical composition, and material hardness testing were preliminary data before the thermomechanics treatment. Then, the thermomechanics treatment was carried out by combining heat treatment and mechanical treatment (plastic deformation) of the Ti-6Al-4V alloy test material. After passing the thermomechanics process, the researchers conducted hardness testing and examination of the microstructure of the Ti-6Al-4V ELI alloy. The data was then analyzed to determine the effect of the thermomechanics process on the hardness value and microstructure changes of the alloy material Ti-6Al-4V.

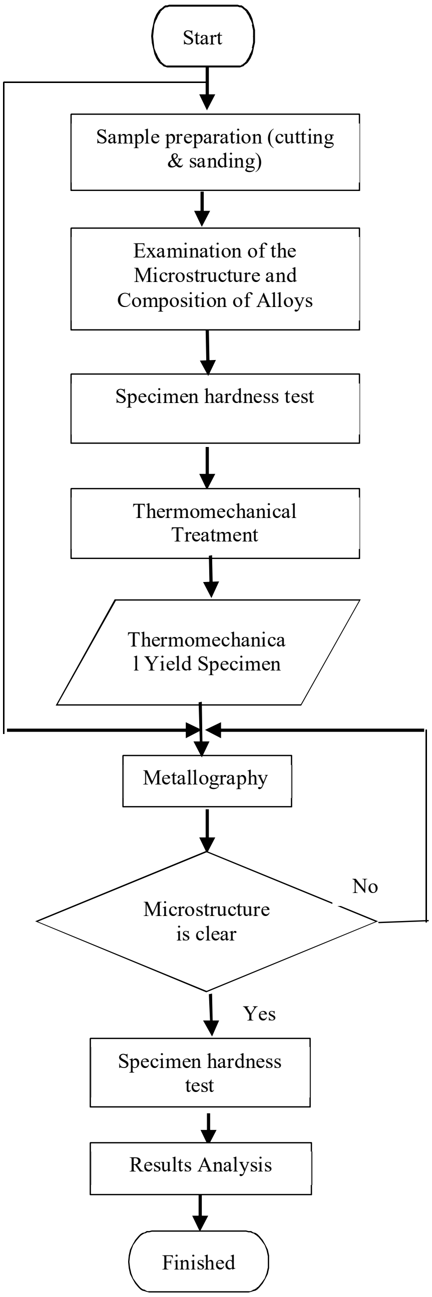

Fig. 2 Research flowchart

III. Results and Discussion

A. Testing the Alloy Ti-6Al-4V ELI Composition

On the Hitachi S-3400N SEM, the Ti-6Al-4V ELI composition was examined by EDX. Figure 3 shows the final results. Based on the results of the spectrum area of composition measurement, Ti-6Al-4V ELI contains Titanium (Ti) 90.01%, Aluminum (Al) 5.54%, and Vanadium (V) 4.45%. The results obtained are in accordance with the standard composition of Ti-6Al-4V ELI, where Aluminum and Vanadium range between 5% - 6.75% and 3.50% - 4.50% [61]. As a result, the specimens used for Ti-6Al-4V ELI met the requirements.

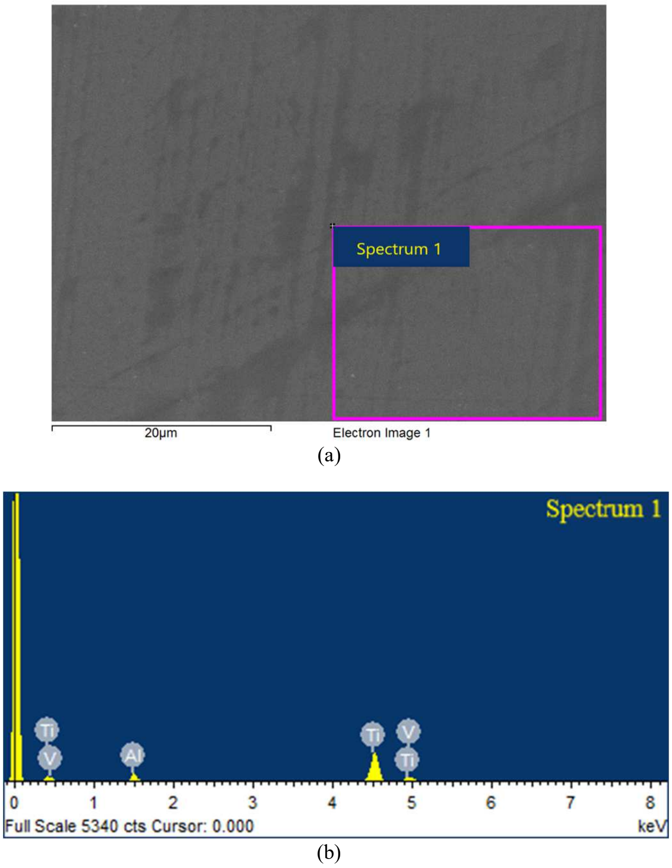

Fig. 3 (a). Ti-6Al-4V ELI composition region (b) Ti-6Al-4V ELI composition spectrum.

B. Ti-6Al-4V ELI Hardness

Each of the five test sites yielded the average hardness of Ti-6Al-4V ELI due to thermomechanical treatment is compared in Table 1. The initial test yielded a hardness of 314 HVN when the alloy was in its as-received state. Previous research indicated that the hardness of Ti-6Al-4V ELI in its as-received condition was nearly identical to Ti-6Al-4V ELI in its as-received condition, i.e., 312 HVN [62]. The beginning state of particular specimens can influence the variation in hardness levels achieved. As demonstrated by measurements of the microstructure of Ti-6Al-4V ELI, previous investigations employed specimens in cast state [62], whereas this study used specimens in mill annealed conditions.

TABLE I
Results of the Ti-6Al-4V ELI Hardness Test

No	As Received	Solution Treatment	10% Deformation	20% Deformation	30% Deformation	Aging Treatment			
						without deformatio	10% Deformatio	20% Deformatio	30% Deformatio
1	316	330	340	368	395	390	390	405	415
2	312	325	345	360	399	385	395	410	419
3	312	337	336	356	392	370	400	408	425
4	311	320	341	358	396	378	398	413	420
5	317	322	347	370	395	381	402	412	428
Mean	314	327	342	362	395	381	397	410	421

The hardness of Ti-6Al-4V ELI raised around 4.14 percent after solution treatment compared to its as-received condition. When the quick cooling procedure (water quenching) took place, the hardness increased due to the creation of the α' martensite phase. Meanwhile, the hardness of Ti-6Al-4V ELI enhanced by around 26.6 percent from its as-received condition in a prior study [62]. Differences in beginning conditions, grain size, and cooling speed can all influence the hardness growth of Ti-6Al-4V ELI. Differences in grain size affect the level of hardness. The larger the grain size, the lower the hardness level. Meanwhile, the higher the cooling speed, the higher the hardness level [60].

Further hardness testing was carried out on Ti-6Al-4V ELI, which had received solution treatment. Ti-6Al-4V ELI, which was given deformation variations of 10%, 20%, and 30%, experienced an increase in hardness from the initial conditions, namely, 8.91%, 15.28%, and 25.79%, respectively. These increases in hardness were in line with the mechanism of strain hardening. The application of plastic deformation caused the dislocations to be deformed and accumulate at the grain boundaries [63]. This buildup made the dislocations more difficult to move, thus requiring higher shear stress to move the dislocations. It resulted in the material's strengthening. The harder Ti-6Al-4V ELI becomes when it is subjected to more plastic deformation (see Figure 4).

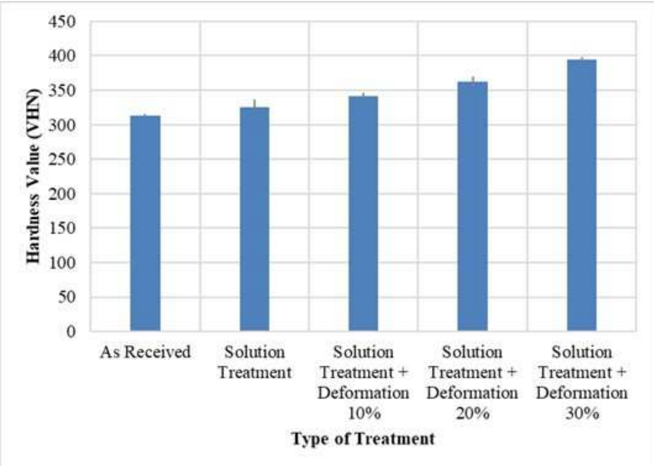

Fig. 4 The hardness of Ti-6Al-4V ELI in its as-received state versus after solution treatment and 10%, 20%, and 30% plastic deformation.

Figure 4 depicts the increase in hardness of Ti-6Al-4V ELI owing to the influence of plastic deformation after solution heat treatment in the form of a graph. Further hardness testing was performed on Ti-6Al-4V ELI after a 1.5-hour aging treatment, which resulted in a 21.33 percent improvement in hardness above the as-received state. According to previous research, aging Ti-6Al-4V for 4 hours increased its hardness by 32.69 percent compared to its original state [62]. The holding duration has an effect on the difference in the rise in hardness of Ti-6Al-4V ELI. The alloy's hardness is influenced by the holding period; the longer the holding time, the higher the alloy's hardness. Over time, however, an excessive amount of holding time might lower the alloy's hardness [60].

The production of fine α phase precipitates from the previous β metastable phase causes the increase in hardness after aging treatment [64]. The precipitation hardening mechanism causes the increase in alloy strength through the formation of fine and evenly distributed phase precipitate particles in the material [63]. The distribution of precipitates on the alloy is carried out through a series of solution treatment processes, namely quenching and aging. The formation of these precipitates through heating is usually called artificial aging.

After subsequent heat treatment, the hardness of Ti-6Al-4V ELI is also affected by plastic deformation following solution treatment (aging treatment). In this work, plastic deformation of 10%, 20%, and 30% enhanced the hardness of Ti-6Al-4V ELI from its as-received condition by 26.43 percent, 30.57 percent, and 34.07 percent, respectively, from its as-received condition. Figure 5 shows the rise in hardness of Ti-6Al-4V ELI following age treatment.

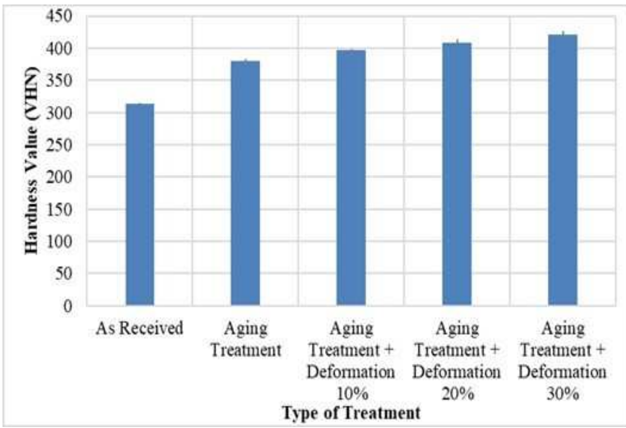

Fig. 5 The hardness of Ti-6Al-4V ELI in its as-received condition against that following age treatment and 10%, 20%, and 30% plastic deformation

More α phase was generated, the Ti-6Al-4V ELI's plastic deformation was increased. This phase in a titanium alloy tends to boost the alloy's strength while having low elasticity, whereas the phase increases the alloy's elasticity [65].

Figure 6 shows how thermomechanical treatment with a combination of solution heat treatment, plastic deformation, and aging treatment increased the Ti-6Al-4V ELI's hardness. The combination of mechanical and solution heat treatment increased the Ti-6Al-4V ELI's hardness; it is shown by the line equation y = 228x + 321.8 or by the hardness equation HVN = 228ε + 321.8, with a correlation coefficient of 0.969. Meanwhile, the increase in hardness in further heat treatment (aging treatment) with a combination of plastic deformation can be expressed by the line equation y = 135x + 381.5 or by the hardness equation HVN = 135ε + 381.5, with a correlation coefficient of 0.991.

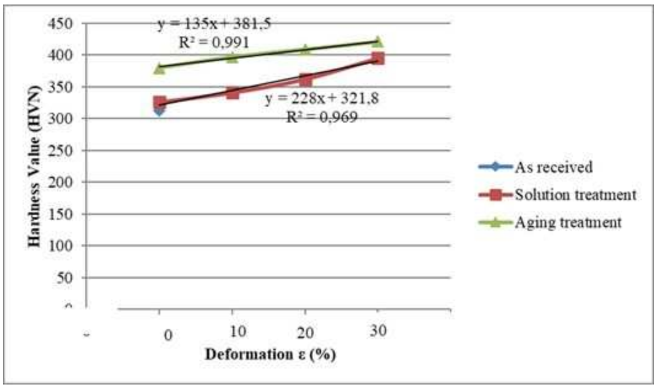

Fig. 6 The influence of the percentage of plastic deformation (ε) on the Ti-6Al-4V ELI's hardness after solution and aging treatment.

C. *Ti-6Al-4V ELI Microstructure*

An Olympus GX71 microscope was used to analyze the microstructure of Ti-6Al-4V ELI. The microstructure was studied under a variety of situations, including as-received, after solution heat treatment, and after aging treatment.

1) Ti-6Al-4V ELI's Microstructure in its as-received condition: Figure 7 shows the results of microstructural observations of Ti-6Al-4V ELI before thermomechanical treatment (in as-received condition).

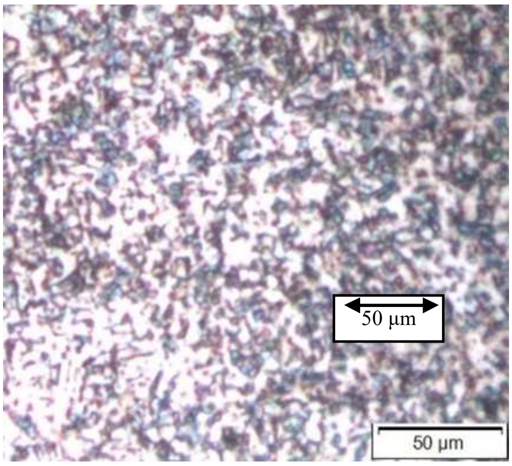

Fig. 7 The findings of observations on the microstructure of Ti-6Al-4V ELI in its as-received state

In Ti-6Al-4V ELI, the phase produced is spherical. The β phase is represented by the dark-colored dots, whereas the brighter sections represent the α phase. Previous research has come up with the same conclusion, namely that the phase generated in the alloy is globular [66]. The mill-annealed state of Ti-6Al-4V ELI was obtained by forming the material at 950°C, annealing it at 700°C for 2 hours, and then slowly cooling it in the open air.

2) Microstructure of Ti-6Al-4V ELI in the solution treatment: Figure 8 indicates the findings of observations on the microstructure of Ti-6Al-4V ELI during solution treatment conditions. The produced phase was martensite, as evidenced by the needle-shaped specimen surface appearance. The β phase changed to a martensite α' phase and then to a fine α phase. At a temperature of 950°C, cooling with water quenching produced an acicular α' martensite microstructure, as well as a primary α and insoluble β phase [62].

A process for dissolving solid alloy atoms into the parent atom to obtain a single phase in the material is known as solution treatment or solid-dissolving mechanism [60]. Water quenching allows for rapid cooling in the $\alpha + \beta$ zone was used to treat the solution on Ti-6Al-4V ELI. Rapid cooling in the $\alpha + \beta$ area led the β phase to change to the α' martensite phase at the particle boundaries, resulting in the β phase, which was not dissolved. When cooled above the β transus temperature (995 °C), the β phase dissolves completely.

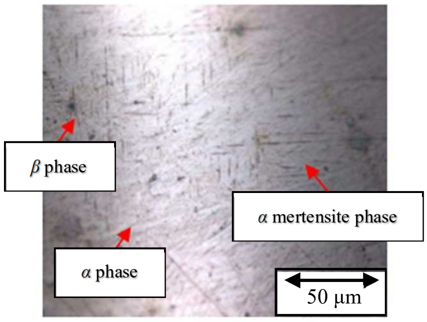

Fig. 8 The Ti-6Al-4V ELI's microstructure was observed under solution treatment conditions, yielding the following results.

After solution treatment, the specimens were stressed with 10%, 20%, and 30% plastic deformation variations at room temperature.

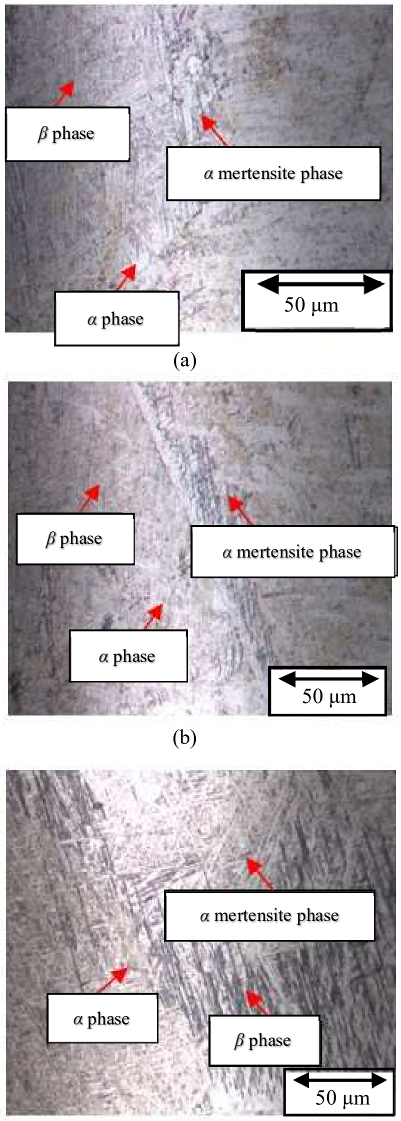

(c)

Fig. 9 After solution treatment at 950°C, the plastic deformation effect on the Ti-6Al-4V's microstructure (a) a ten percent distortion (b) a 20 percent distortion (c) Deformation of 30 percent

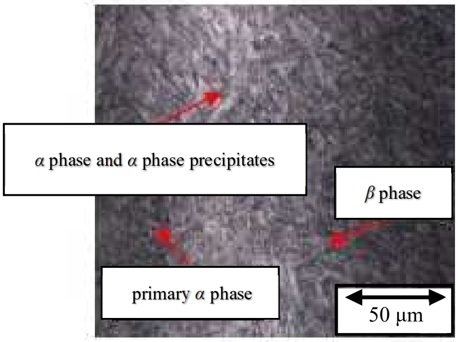

(a)

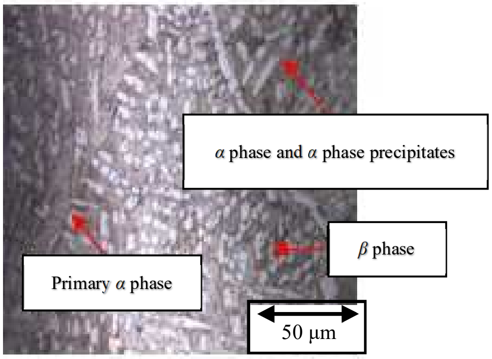

(b)

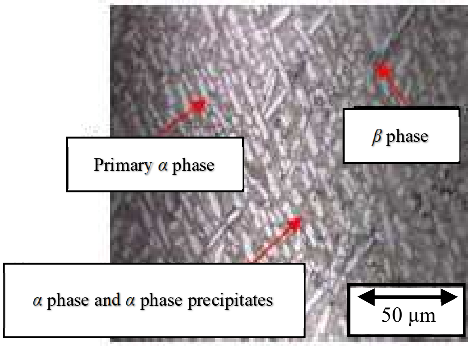

(c)

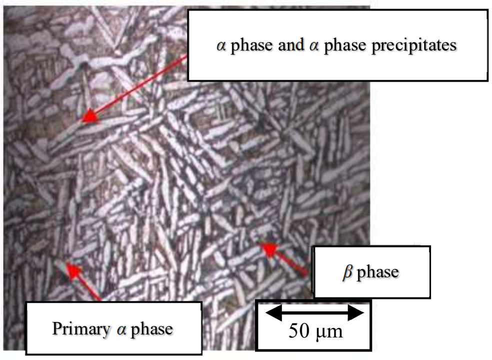

(d)

Fig. 10 The effect of Ti-6Al-4V's plastic deformation in solution on the aging process. (a) unaffected by deformation (b) (a) 10% (b) 20% (c) 30% (d) 40%.

Figure 9 depicts the impact of plastic deformation on the Ti-6Al-4V ELI's microstructure after 950ºC solution treatment. Plastic deformation did not affect the solution-treated Ti-6Al-4V ELI phase, but it did cause the Ti-6Al-4V ELI grains to split, resulting in the recrystallization phenomena [63]. The martensitic structure of Ti-6Al-4V ELI was influenced by the deformation applied. The tightening of the martensitic structure of the alloy was driven by increased plastic deformation.

3) Ti-6Al-4V ELI microstructure under aging treatment: The microstructure in Figure 10 was created by aging at 550ºC for 1.5 hours with a holding duration of 15 minutes. After a solution heat treatment at 950ºC, aging treatment resulted in a phase transition from α' martensite to $\alpha + \beta$. At the grain boundaries of Ti-6Al-4V, the phase expanded and evolved. In Ti-6Al-4V grains, however, the α' phase and the α phase precipitate developed. The recrystallization mechanism influenced the formation of the phase after aging treatment and deformation changes. The easier it is for recrystallization to occur at a given plastic deformation [63]. The α phase causes the alloy to become stronger, and the Ti-6Al-4V's plastic deformation becomes higher [64].

IV. Conclusion

This study showed that the thermomechanical treatment could increase the hardness value of Ti-6Al-4V ELI and change its microstructure, indicating an increase in the α phase. The increase in the hardness value of Ti-6Al-4V can be expressed by the equation HVN = 135ε + 381.5, with a correlation coefficient of 0.991. The increase in the α phase due to deformation also affected the material to become stronger.

Acknowledgment

The corresponding author thanks the Directorate General Higher Education, Ministry of Education, Culture, Research and Technology, Republic of Indonesia for financial support under Basic Research Grant with contract no. T/31/UN.16.17/PT.01.03/PD-Material Maju/2021.

References

[1] M. Abdel-Hady Gepreel and M. Niinomi, "Biocompatibility of Ti-alloys for long-term implantation," *J. Mech. Behav. Biomed. Mater.*, vol. 20, pp. 407–415, 2013, doi: 10.1016/j.jmbbm.2012.11.014.

[2] J. A. Disegi and L. Eschbach, "Stainless steel in bone surgery," *Injury*, vol. 31, no. SUPPL. 4, 2000, doi: 10.1016/S0020-1383(00)80015-7.

[3] M. Niinomi, "Biologically and Mechanically Biocompatible Titanium Alloys Ti-6Al-4V ELI," vol. 49, no. 10, pp. 2170–2178, 2008, doi: 10.2320/matertrans.L-MRA2008828.

[4] A. Ajiz, Gunawarman, and J. Affi, "The effects of short-time solution treatment and short-time aging on mechanical properties of Ti-6Al-4V for orthopaedic applications," *Int. J. Adv. Sci. Eng. Inf. Technol.*, vol. 5, no. 4, pp. 329–334, 2015, doi: 10.18517/ijaseit.5.4.556.

[5] M. Niinomi, D. Eylon, S. Fujishiro, and C. Ouchi, "Effect of b Phase Stability at Room Temperature on Mechanical Properties in b -Rich a ⁄ b Type Ti – 4 . 5Al – 3V – 2Mo – 2Fe Alloy," vol. 42, no. 2, pp. 191–199, 2002.

[6] Y. F. Xu, D. Q. Yi, H. Q. Liu, X. Y. Wu, B. Wang, and F. L. Yang, "Effects of cold deformation on microstructure, texture evolution and mechanical properties of Ti-Nb-Ta-Zr-Fe alloy for biomedical applications," *Mater. Sci. Eng. A*, vol. 547, pp. 64–71, 2012, doi: 10.1016/j.msea.2012.03.081.

[7] S. Anderson, Annisa, J. Affi, Y. Yetri, and G. Gunawarman, "The Effect of Aging Treatment on Mechanical Properties and Microstructures of Ti-12Cr in Ortodontic Applications," *IOP Conf. Ser. Mater. Sci. Eng.*, vol. 846, no. 1, 2020, doi: 10.1088/1757-899X/846/1/012066.

[8] T. Akahori, M. Niinomi, H. Fukui, and A. Suzuki, "Fatigue, fretting fatigue and corrosion characteristics of biocompatible beta type titanium alloy conducted with various thermo-mechanical treatments," *Mater. Trans.*, vol. 45, no. 5, pp. 1540–1548, 2004, doi: 10.2320/matertrans.45.1540.

[9] J. Yang, H. Yang, H. Yu, Z. Wang, and X. Zeng, "Corrosion Behavior of Additive Manufactured Ti-6Al-4V Alloy in NaCl Solution," *Metall. Mater. Trans. A Phys. Metall. Mater. Sci.*, vol. 48, no. 7, pp. 3583–3593, 2017, doi: 10.1007/s11661-017-4087-9.

[10] B. Wu, Z. Pan, S. Li, D. Cuiuri, D. Ding, and H. Li, "The anisotropic corrosion behaviour of wire arc additive manufactured Ti-6Al-4V alloy in 3.5% NaCl solution," *Corros. Sci.*, vol. 137, no. August 2017, pp. 176–183, 2018, doi: 10.1016/j.corsci.2018.03.047.

[11] Y. Xu, Y. Lu, J. Liang, and R. D. Sisson, "Microstructure and corrosion behaviour of additively manufactured Ti–6Al–4V with various post-heat treatments," *Mater. Sci. Technol. (United Kingdom)*, vol. 35, no. 1, pp. 89–97, 2019, doi: 10.1080/02670836.2018.1542052.

[12] S. Gnanavel, S. Ponnusamy, L. Mohan, and C. Muthamizhchelvan, "In Vitro Corrosion Behaviour of Ti–6Al–4V and 316L Stainless Steel Alloys for Biomedical Implant Applications," *J. Bio- Tribo-Corrosion*, vol. 4, no. 1, pp. 4–11, 2018, doi: 10.1007/s40735-017-0118-8.

[13] S. Carquigny, J. Takadoum, and S. Ivanescu, "Corrosion and tribocorrosion study of 316L steel, Ti–6Al–4V and Ti–10Zr–10Nb–5Ta," *Tribol. - Mater. Surfaces Interfaces*, vol. 13, no. 2, pp. 112–119, 2019, doi: 10.1080/17515831.2019.1596625.

[14] M. Sarraf *et al.*, "In vitro bioactivity and corrosion resistance enhancement of Ti-6Al-4V by highly ordered TiO 2 nanotube arrays," *J. Aust. Ceram. Soc.*, vol. 55, no. 1, pp. 187–200, 2019, doi: 10.1007/s41779-018-0224-1.

[15] N. Hu *et al.*, "Homogeneous Anodic TiO2 Nanotube Layers on Ti–6Al–4V Alloy with Improved Adhesion Strength and Corrosion Resistance," *Adv. Mater. Interfaces*, vol. 6, no. 12, pp. 1–12, 2019, doi: 10.1002/admi.201801964.

[16] M. Nabhani, R. Shoja Razavi, and M. Barekat, "Corrosion study of laser cladded Ti-6Al-4V alloy in different corrosive environments," *Eng. Fail. Anal.*, vol. 97, no. December 2018, pp. 234–241, 2019, doi: 10.1016/j.engfailanal.2019.01.023.

[17] Y. Bai *et al.*, "Improved corrosion behaviour of electron beam melted Ti-6Al–4V alloy in phosphate buffered saline," *Corros. Sci.*, vol. 123, pp. 289–296, 2017, doi: 10.1016/j.corsci.2017.05.003.

[18] L. C. Campanelli, C. C. Bortolan, P. S. C. P. da Silva, C. Bolfarini, and N. T. C. Oliveira, "Effect of an amorphous titania nanotubes coating on the fatigue and corrosion behaviors of the biomedical Ti-6Al-4V and Ti-6Al-7Nb alloys," *J. Mech. Behav. Biomed. Mater.*, vol. 65, pp. 542–551, 2017, doi: 10.1016/j.jmbbm.2016.09.015.

[19] S. Bose, L. C. Pathak, and R. Singh, "Response of boride coating on the Ti-6Al-4V alloy to corrosion and fretting corrosion behavior in Ringer's solution for bio-implant application," *Appl. Surf. Sci.*, vol. 433, pp. 1158–1174, 2018, doi: 10.1016/j.apsusc.2017.09.223.

[20] S. Baragetti and E. V. Arcieri, "Corrosion fatigue behavior of Ti-6Al-4 V: Chemical and mechanical driving forces," *Int. J. Fatigue*, vol. 112, pp. 301–307, 2018, doi: 10.1016/j.ijfatigue.2018.02.033.

[21] T. M. Chiu, M. Mahmoudi, W. Dai, A. Elwany, H. Liang, and H. Castaneda, "Corrosion assessment of Ti-6Al-4V fabricated using laser powder-bed fusion additive manufacturing," *Electrochim. Acta*, vol. 279, pp. 143–151, 2018, doi: 10.1016/j.electacta.2018.04.189.

[22] G. A. Longhitano *et al.*, "Heat treatments effects on functionalization and corrosion behavior of Ti-6Al-4V ELI alloy made by additive manufacturing," *J. Alloys Compd.*, vol. 765, pp. 961–968, 2018, doi: 10.1016/j.jallcom.2018.06.319.

[23] Q. Zhang, B. Duan, Z. Zhang, J. Wang, and C. Si, "Effect of ultrasonic shot peening on microstructure evolution and corrosion resistance of selective laser melted Ti-6Al-4V alloy," *J. Mater. Res. Technol.*, vol. 11, pp. 1090–1099, 2021, doi: 10.1016/j.jmrt.2021.01.091.

[24] S. Kumar, V. Pandey, K. Chattopadhyay, and V. Singh, "Surface Nanocrystallization Induced by Ultrasonic Shot Peening and Its Effect on Corrosion Resistance of Ti–6Al–4V Alloy," *Trans. Indian Inst. Met.*, vol. 72, no. 3, pp. 789–792, 2019, doi: 10.1007/s12666-018-1531-5.

[25] F. M. Kgoete, A. P. I. Popoola, and O. S. I. Fayomi, "Influence of spark plasma sintering on microstructure and corrosion behaviour of Ti-6Al-4V alloy reinforced with micron-sized Si3N4 powder," *Def. Technol.*, vol. 14, no. 5, pp. 403–407, 2018, doi: 10.1016/j.dt.2018.04.011.

[26] M. Chellappa and U. Vijayalakshmi, "Electrophoretic deposition of silica and its composite coatings on Ti-6Al-4V, and its in vitro corrosion behaviour for biomedical applications," *Mater. Sci. Eng. C*, vol. 71, pp. 879–890, 2017, doi: 10.1016/j.msec.2016.10.075.

[27] R. Yazdi, H. M. Ghasemi, C. Wang, and A. Neville, "Bio-corrosion behaviour of oxygen diffusion layer on Ti-6Al-4V during tribocorrosion," *Corros. Sci.*, vol. 128, pp. 23–32, 2017, doi: 10.1016/j.corsci.2017.08.031.

[28] J. Fojt *et al.*, "Corrosion behaviour and cell interaction of Ti-6Al-4V alloy prepared by two techniques of 3D printing," *Mater. Sci. Eng. C*, vol. 93, no. January, pp. 911–920, 2018, doi: 10.1016/j.msec.2018.08.066.

[29] A. A. Rozali, N. R. N. Masdek, M. C. Murad, Z. Salleh, and K. M. Hyie, "The effect of pH value on the corrosion behaviour of Ti-6Al-4V and 316L SS alloys under physiological environment," *Chem. Eng. Trans.*, vol. 63, pp. 769–774, 2018, doi: 10.3303/CET1863129.

[30] Y. Xu, J. Wang, X. Zhang, P. Wang, J. Shi, and F. Huo, "Corrosion behaviour of Ti-6Al-4V alloy as dental implant containing fluoride ions," *Int. J. Electrochem. Sci.*, vol. 12, no. 11, pp. 10308–10316, 2017, doi: 10.20964/2017.11.04.

[31] A. C. Hee *et al.*, "Corrosion behaviour and microstructure of tantalum film on Ti6Al4V substrate by filtered cathodic vacuum arc deposition," *Thin Solid Films*, vol. 636, pp. 54–62, 2017, doi: 10.1016/j.tsf.2017.05.030.

[32] M. Buciumeanu *et al.*, "Study of the tribocorrosion behaviour of Ti6Al4V – HA biocomposites," *Tribol. Int.*, vol. 107, pp. 77–84, 2017, doi: 10.1016/j.triboint.2016.11.029.

[33] X. Gong *et al.*, "Building direction dependence of corrosion resistance property of Ti–6Al–4V alloy fabricated by electron beam melting," *Corros. Sci.*, vol. 127, pp. 101–109, 2017, doi: 10.1016/j.corsci.2017.08.008.

[34] O. Heintz, V. Vignal, H. Krawiec, and J. Loch, "Passivity and corrosion behaviour of Ti-10Mo-4Zr and Ti-6Al-4V alloys after long-term ageing in Ringer's solution at 37 °C," *J. Solid State Electrochem.*, vol. 21, no. 5, pp. 1445–1455, 2017, doi: 10.1007/s10008-017-3506-6.

[35] P. Chandramohan, S. Bhero, B. A. Obadele, and P. A. Olubambi, "Laser additive manufactured Ti–6Al–4V alloy: tribology and corrosion studies," *Int. J. Adv. Manuf. Technol.*, vol. 92, no. 5–8, pp. 3051–3061, 2017, doi: 10.1007/s00170-017-0410-2.

[36] V. Pejaković, V. Totolin, and M. Rodríguez Ripoll, "Tribocorrosion behaviour of Ti6Al4V in artificial seawater at low contact pressures," *Tribol. Int.*, vol. 119, no. October 2017, pp. 55–65, 2018, doi: 10.1016/j.triboint.2017.10.025.

[37] L. Zhang, J. Xu, B. Chen, H. Yu, and Z. Lian, "Microhardness and corrosion resistance behaviour of Ti-6Al-4V alloy-coloured surface under WEDM-HS process," *Micro Nano Lett.*, vol. 12, no. 9, pp. 618–623, 2017, doi: 10.1049/mnl.2017.0037.

[38] J. J. de Damborenea, M. A. Arenas, M. A. Larosa, A. L. Jardini, C. A. de Carvalho Zavaglia, and A. Conde, "Corrosion of Ti6Al4V pins produced by direct metal laser sintering," *Appl. Surf. Sci.*, vol. 393, pp. 340–347, 2017, doi: 10.1016/j.apsusc.2016.10.031.

[39] Y. Zhang, O. Addison, F. Yu, B. C. R. Troconis, J. R. Scully, and A. J. Davenport, "Time-dependent Enhanced Corrosion of Ti6Al4V in the Presence of H2O2 and Albumin," *Sci. Rep.*, vol. 8, no. 1, pp. 1–11, 2018, doi: 10.1038/s41598-018-21332-x.

[40] J. Li *et al.*, "Electrochemical corrosion, wear and cell behavior of ZrO2/TiO2 alloyed layer on Ti-6Al-4V," *Bioelectrochemistry*, vol. 121, pp. 105–114, 2018, doi: 10.1016/j.bioelechem.2018.01.011.

[41] K. Soorya Prakash, P. M. Gopal, D. Anburose, and V. Kavimani, "Mechanical, corrosion and wear characteristics of powder metallurgy processed Ti-6Al-4V/B4C metal matrix composites," *Ain Shams Eng. J.*, vol. 9, no. 4, pp. 1489–1496, 2018, doi: 10.1016/j.asej.2016.11.003.

[42] G. Rasool, Y. El Shafei, and M. M. Stack, "Mapping tribo-corrosion behaviour of TI-6AL-4V eli in laboratory simulated hip joint environments," *Lubricants*, vol. 8, no. 7, 2020, doi: 10.3390/LUBRICANTS8070069.

[43] L. Semetse, B. A. Obadele, L. Raganya, J. Geringer, and P. A. Olubambi, "Fretting corrosion behaviour of Ti-6Al-4V reinforced with zirconia in foetal bovine serum," *J. Mech. Behav. Biomed. Mater.*, vol. 100, no. January, p. 103392, 2019, doi: 10.1016/j.jmbbm.2019.103392.

[44] J. Dai, H. Zhang, C. Sun, S. Li, C. Chen, and Y. Yang, "The effect of Nb and Si on the hot corrosion behaviors of TiAl coatings on a Ti-6Al-4V alloy," *Corros. Sci.*, vol. 168, no. February, p. 108578, 2020, doi: 10.1016/j.corsci.2020.108578.

[45] B. Pazhanivel, P. Sathiya, and G. Sozhan, "Ultra-fine bimodal ($\alpha + \beta$) microstructure induced mechanical strength and corrosion resistance of Ti-6Al-4V alloy produced via laser powder bed fusion process," *Opt. Laser Technol.*, vol. 125, no. October 2019, p. 106017, 2020, doi: 10.1016/j.optlastec.2019.106017.

[46] O. S. Adesina, B. A. Obadele, G. A. Farotade, D. A. Isadare, A. A. Adediran, and P. P. Ikubanni, "Influence of phase composition and microstructure on corrosion behavior of laser based Ti–Co–Ni ternary

coatings on Ti–6Al–4V alloy," *J. Alloys Compd.*, vol. 827, p. 154245, 2020, doi: 10.1016/j.jallcom.2020.154245.
[47] Q. Sui *et al.*, "Effect of build orientation on the corrosion behavior and mechanical properties of selective laser melted Ti-6Al-4V," *Metals (Basel).*, vol. 9, no. 9, 2019, doi: 10.3390/met9090976.
[48] P. Bocchetta, L. Y. Chen, J. D. C. Tardelli, A. C. Dos Reis, F. Almeraya-Calderón, and P. Leo, "Passive layers and corrosion resistance of biomedical ti-6al-4v and β-ti alloys," *Coatings*, vol. 11, no. 5, 2021, doi: 10.3390/coatings11050487.
[49] P. Qin *et al.*, "Corrosion and passivation behavior of laser powder bed fusion produced Ti-6Al-4V in static/dynamic NaCl solutions with different concentrations," *Corros. Sci.*, vol. 191, no. May, p. 109728, 2021, doi: 10.1016/j.corsci.2021.109728.
[50] X. Zhou *et al.*, "Microstructural evolution and corrosion behavior of Ti–6Al–4V alloy fabricated by laser metal deposition for dental applications," *J. Mater. Res. Technol.*, vol. 14, no. Lmd, pp. 1459–1472, 2021, doi: 10.1016/j.jmrt.2021.07.006.
[51] L. Y. Chen *et al.*, "Corrosion behavior and characteristics of passive films of laser powder bed fusion produced Ti–6Al–4V in dynamic Hank's solution," *Mater. Des.*, vol. 208, p. 109907, 2021, doi: 10.1016/j.matdes.2021.109907.
[52] S. Nisaimun, P. Poolcharuansin, P. Visuttipitukul, and P. Klomjit, "Improving corrosion resistance of 3D printed Ti-6Al-4V by TiN coating," *J. Met. Mater. Miner.*, vol. 31, no. 2, pp. 137–146, 2021, doi: 10.14456/jmmm.2021.31.
[53] J. Cheng *et al.*, "Corrosion behavior of As-Cast Ti–10Mo–6Zr–4Sn–3Nb and Ti–6Al–4B in hank's solution: A comparison investigation," *Metals (Basel).*, vol. 11, no. 1, pp. 1–15, 2021, doi: 10.3390/met11010011.
[54] J. V. de Sousa Araujo *et al.*, "Thermomechanical treatment and corrosion resistance correlation in the AA2198 Al–Cu–Li alloy," *Corros. Eng. Sci. Technol.*, vol. 54, no. 7, pp. 575–586, 2019, doi: 10.1080/1478422X.2019.1637077.
[55] D. Yuan, J. Wang, H. Chen, W. Xie, H. Wang, and B. Yang, "Mechanical properties and microstructural evolution of a Cu–Cr–Ag alloy during thermomechanical treatment," *Mater. Sci. Technol. (United Kingdom)*, vol. 34, no. 12, pp. 1433–1440, 2018, doi: 10.1080/02670836.2018.1459094.
[56] B. Mishra, D. Vijay Kumar, C. Pakhare, K. N. Jonnalagadda, and M. J. N. V. Prasad, "Effect of thermomechanical processing on microstructural evolution and deformation behaviour of polycrystalline magnesium under quasi-static and high strain rate conditions," *Philos. Mag.*, vol. 97, no. 14, pp. 1071–1087, 2017, doi: 10.1080/14786435.2017.1290294.
[57] S. Tonpe and U. Kamachi Mudali, "Effect of thermomechanical process on microstructural evolution, mechanical and corrosion properties of zircaloy-4 tubes of mock-up dissolver vessel," *Mater. Manuf. Process.*, vol. 32, no. 1, pp. 27–33, 2017, doi: 10.1080/10426914.2015.1090589.
[58] M. Motyka and J. Sieniawski, "The influence of initial plastic deformation on microstructure and hot plasticity of α+β titanium alloys," *Arch. Mater. Sci. Eng.*, vol. 41, no. 2, pp. 95–103, 2010.
[59] P. West Conshohocken, *ASTM 348. Standard Test Methods for Knoop and Vickers hardness materials.*
[60] W. D. Callister, "Materials science and engineering: An introduction (2nd edition)," *Mater. Des.*, vol. 12, no. 1, p. 59, 1991, doi: 10.1016/0261-3069(91)90101-9.
[61] Welsch, Gerhard, Rodney Boyer, and E. W. Collings, eds. Materials properties handbook: titanium alloys. ASM international, 1993.
[62] T. Trnava, S. Republic, and B. Polytechnic, "The influence of heat treatment on the microstructure of the casted ti6al4v titanium alloy," *Mater. World*, vol. 2, pp. 1–6, 2007.
[63] G. Gunawarman, *). Konsep dan Teori Metalurgi Fisik. Yogyakarta (ID): Andi Offset*. 2013.
[64] R. K. Gupta, V. A. Kumar, C. Mathew, and G. S. Rao, "Strain hardening of Titanium alloy Ti6Al4V sheets with prior heat treatment and cold working," *Mater. Sci. Eng. A*, vol. 662, pp. 537–550, 2016, doi: 10.1016/j.msea.2016.03.094.
[65] R. Reda, A. A. Nofal, and A. A. Hussein, "Effect of Quenching Temperature on the Mechanical Properties of Cast Ti-6Al-4V Alloy," *www.me-journal.org J. Metall. Eng.*, vol. 2, no. 1, pp. 48–54, 2013.
[66] F. J. Gil, M. P. Ginebra, J. M. Manero, and J. A. Planell, "Formation of α-Widmanstätten structure: Effects of grain size and cooling rate on the Widmanstätten morphologies and on the mechanical properties in Ti6Al4V alloy," *J. Alloys Compd.*, vol. 329, no. 1–2, pp. 142–152, 2001, doi: 10.1016/S0925-8388(01)01571-7.